PHYSICAL REVIEW A VOLUME 43, NUMBER 2 15 JANUARY 1991

Escaped-radial nematic configuration in submicrometer-size cylindrical cavities: Deuterium nuclear-magnetic-resonance study

G. P. Crawford, M. Vilfan,* and J. W. Doane
Liquid Crystal Institute and Department of Physics, Kent State University, Kent, OH 44242-0001

I. Vilfan
J. Stefan Institute, Jamova 39, Ljubljana, Yugoslavia
(Received 17 August 1990)

Deuterium nuclear magnetic resonance (^{2}H NMR) is used to extend studies of confined nematic structures to submicrometer-size cavities. Spectral patterns reveal the escaped-radial configuration in untreated cylindrical cavities of Nuclepore filters. This configuration is found to survive in pore sizes as small as 0.2 μm in radius. Singular point defects are found to be present along the escape axis with the density of the defects being determined from the ^{2}H NMR spectra. This density is found to be unaffected by cycling between the nematic and isotropic phases with or without the presence of an applied magnetic field.

I. INTRODUCTION

It was theoretically predicted in the early 1970s that the nematic director field in a cylindrical cavity with homeotropic-type boundary conditions could be a pure radial configuration with a line disclination along the cylinder axis.[1] This structure involves a core in the center of the cylinder where the director field is undefined. Cladis and Kleman[2] as well as Meyer[3] have shown that another configuration is more stable for cylinders larger than 0.1 μm in diameter where the disclination line escapes into the third dimension along the cylinder axis. This arrangement of the director field is continuous and involves no core defect. Optical studies of nematic liquid crystals in large cylindrical cavities with radii of 20–200 μm have verified the existence of the "escaped-radial" structure.[3–6] Singular point defects in the escaped configuration were revealed in the optical studies.[5] These singular points were found to be of two types which alternate along the axis of the cylinder and result from the fact that two energetically equivalent configurations exist where the direction of bend is changed. Observation of the escaped-radial configuration was extended to smaller cylindrical cavity sizes by Kuzma and Labes[7] but optical methods are limited to cavity radii $\sim$2–3 μm, far larger than the size expected ($\leq$0.1 μm) where elastic energies become favorable to induce other kinds of configurations[2] as well as perhaps compete with surface anchoring energies.[8]

In this paper we show how these configuration studies can be extended to submicrometer-size cavities using deuterium nuclear magnetic resonance (^{2}H NMR). We report the first experimental studies of the nematic director configuration in cylindrical cavities of radii 0.3 and 0.2 μm demonstrating the effectiveness of this technique in observing nematic configurations in high detail to the point of even identifying and studying singular defect structures and their densities. Our experimental studies are carried out in the cylindrical pores of polycarbonate Nuclepore membranes that were permeated with the deuterated liquid crystal compound 4'-pentyl-4-cyanobiphenyl (5CB-βd_2). The high density of pores in the membranes allows this study to be accessible with nuclear magnetic resonance techniques.

In the ^{2}H NMR technique the nematic director configuration is directly obtained from the shape of the spectral pattern. Spectral patterns reveal the profile of the structure for different orientations of the cylinder axis projected along the magnetic-field direction of the NMR spectrometer, allowing for precise director structure determination. Translational diffusion is shown to also affect the spectral pattern, but in the sizes reported here, the effect is small and negligible. Likewise, the cavities sizes studied are too small for the magnetic field of the spectrometer to affect the director configuration. We found the escaped-radial configuration to be present in the submicron-size cavities studied but with singular point defects along the escape axis. A value for the density of these defects is measured to be $L/R = 2 \pm 0.5$ where L is the separation between defects and R is the radius of the cylinder. This density is found to be unaffected by different sample-preparation methods.

II. NEMATIC DIRECTOR CONFIGURATIONS IN CYLINDRICAL CAVITIES

A nematic liquid crystal confined to a cylindrical environment exhibits a specific director configuration resulting from an interplay between elastic forces, a possible external field, morphology and size of cavity, and surface interactions. The deformation free energy of a liquid crystal confined to a cylindrical cavity in the constant order parameter and strong anchoring approximations as well as avoiding twist deformation can be expressed as[1]

$$F=\tfrac{1}{2}\int_{\text{vol}}\left[K_{11}(\nabla\cdot\mathbf{n})^2+K_{33}(\mathbf{n}\times\nabla\times\mathbf{n})^2 - \frac{\Delta\chi}{\mu_0}(\mathbf{n}\cdot\mathbf{B})^2\right]dV\ , \tag{1}$$

where the first two terms describe the elastic deformations of the liquid crystal in the cylinder. K_{11} and K_{33} are elastic constants associated with splay and bend deformations, respectively. The third term incorporates the influence of the magnetic field where $\Delta\chi$ is the anistropy of the diamagnetic susceptibility. The importance of the field term can be estimated by calculating the coherence length ξ_m given by the equation

$$\xi_m \simeq \left[\frac{\mu_0 K}{\Delta\chi}\right]^{1/2}\frac{1}{B}\ , \tag{2}$$

where K can be either K_{11}, K_{33}, or a combination of these elastic constants, depending upon the specific director configuration. In our experiments the 4.7 T magnetic field of the NMR spectrometer produces a coherence length of $\xi_m \simeq 1.7$ μm, which is larger than the radii of the cylindrical cavities to be studied here. Because of this, the field term has a small effect and, as will be shown later, can be neglected in our studies.

Assuming strong anchoring of the nematic director in a direction perpendicular to the surface of a cylindrical cavity, Dzyaloshinskii[1] found that the total free energy of Eq. (1) could be minimized for a director configuration which has only a radial component in a plane perpendicular to the cylinder axis, resulting in a pure splay deformation energy with a line disclination at the center of the cylinder illustrated in Fig. 1(a). Subsequently, Cladis and Kleman[2] have shown that with perpendicular anchoring at the surface, the total energy may be reduced by eliminating the line disclination and allowing the molecules to relax out of the plane. Therefore, the divergence in the splay energy is avoided by including a finite amount of bend deformation as the disclination escapes into the third dimension. The energy of the escape configuration is independent of the cylinder radius. A solution of the minimization criteria for the free energy for the case when $K_{11}=K_{33}$ is given by

$$\phi(\rho)=\sin^{-1}\left[\frac{R^2-\rho^2}{R^2+\rho^2}\right]\ , \tag{3}$$

where R is the radius of the cylinder, ρ is the local position in cylindrical coordinates of the nematic director, and ϕ is the angle between the director and its projection on the cylinder cross section.[2] The director configuration resulting from Eq. (3) is calculated and illustrated in Fig. 1(b). For $K_{11}<K_{33}$, where no twist is allowed, the solution is expressed by

$$\frac{\rho}{R}=\left[\frac{\cos k\ \sin\phi-(1-\sin^2 k\ \sin^2\phi)^{1/2}}{\cos k\ \sin\phi+(1-\sin^2 k\ \sin^2\phi)^{1/2}}\right]^{1/2} \times\exp\left[-\tan(k)\sin^{-1}(\sin k\ \sin\phi)\right]\ , \tag{4}$$
$$k=\tan^{-1}\left[\frac{K_{33}-K_{11}}{K_{11}}\right]\ .$$

Figure 1(c) illustrates the director configuration for the case when $K_{33}/K_{11}=5$, resulting in a slower increase in the director field in the z direction as $\rho\rightarrow 0$. Cladis and Kleman have also presented solutions for the circular configuration with tangential surface anchoring where the nematic director can relax out of the plane, avoiding any splay deformations, resulting in a complex twist-bend configuration. This has been experimentally observed in large capillaries[9] but will not be considered further in this contribution.

We have considered equations similar to those of Cladis and Kleman for the escaped-radial structure, but have included the influence of the magnetic field and singular point defects resulting from the encounter of two opposing escape domains. Point defects are included in the escaped-radial configuration by applying homeotropic boundary conditions at the cylinder walls and incorporat-

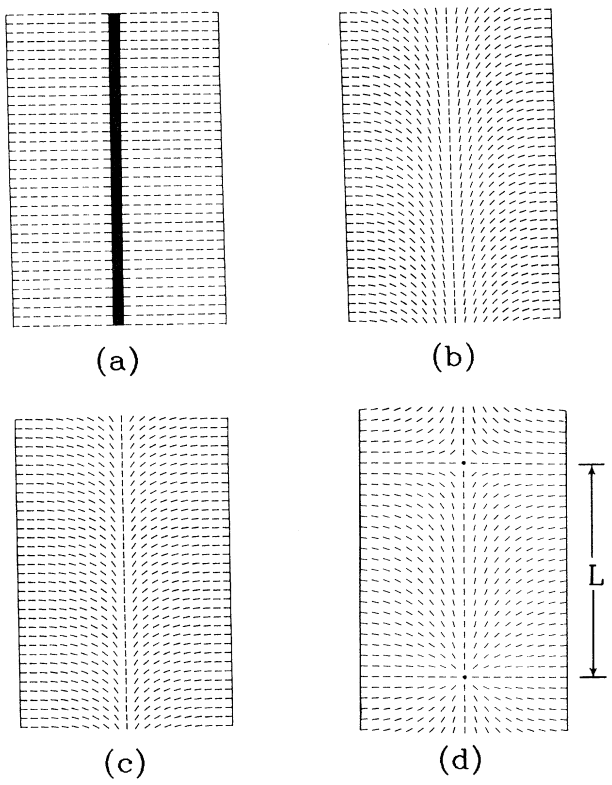

FIG. 1. Illustrations of nematic director configurations with homeotropic-type boundary conditions for the pure radial configuration with an exaggerated core defect (a), the escaped-radial configuration for $K_{33}/K_{11}=1.0$ (b), $K_{33}/K_{11}=5.0$ (c), and the escaped-radial configuration with singular point defects separated by a distance L for $K_{33}/K_{11}=1.0$ (d).

ing a planar radial distribution of molecules in several planes a finite distance L apart.[10] The resulting structure is numerically calculated and presented in Fig. 1(d). The radial planes of molecules or domain walls carry an additional free energy due to the point defects. It can be calculated[10] that the interaction between domain walls is attractive for small L ($L/R \leq 0.25$) and repulsive for larger L/R. This means that the domain walls annihilate when they are closer than $L/R=0.25$. For $L/R \geq 0.25$ they will repel but cannot disappear at the open surface of the cylinder because of another repulsive interaction between the domain wall and the surface. Thus any structure with the domain-wall separation $L/R \geq 0.25$ is metastable and does not change in time in the sample.

III. DEUTERIUM NMR LINE SHAPES

The characteristic features of the spectral line shapes that are important in our studies of a nematic liquid crystal confined to cylindrical cavities are the width and shape of the spectral patterns. In the constant-order parameter approximation throughout the volume of the cylinder for a uniaxial liquid crystal, the line shape and linewidth essentially depend on three factors: the nematic director configuration inside the cylinder, the orientation of the cylinder with respect to the magnetic field, and the translational molecular self-diffusion constant. Since the resonance frequency depends on the angle between the nematic director and the external field, the ^{2}H-NMR spectral pattern is a direct indication of the nematic director configuration inside the cylindrical cavity. The orientation of the cylinder can be changed in the magnetic field to give the profile of the configuration projected in different directions. The effect of translational diffusion on the spectra depends on the cylinder size and the quadrupole splitting. Using typical values of the diffusion constant $D \sim 10^{-11}$ m^2/s, the extent of motional averaging can be estimated by the relation $d \sim (D/\delta\nu)^{1/2}$. For spectra with a quadrupole splitting, $\delta\nu = 10$ kHz, the distance d a molecule diffuses on the average is ~ 0.03 μm, which is substantially smaller than the radius of the cylindrical cavities studied. Diffusion, therefore, has a small effect and will be shown later to be negligible.

In a local region represented by the position vector $\mathbf{r}$, a compound deuterated at a specific site will yield a spectrum of two lines at angular quadrupole frequencies ω_q, given by the expression

$$\omega_q(\mathbf{r}) = \pm\pi\frac{\delta\nu}{2}\left[3\cos^2\theta(\mathbf{r})-1\right], \tag{5}$$

where $\theta(\mathbf{r})$ expresses the orientation of the local nematic director relative to the magnetic field, $\delta\nu$ is the quadrupole splitting in the bulk nematic phase given by $3e^2qQS/2h$, eq is the electric-field gradient created by the carbon-deuterium (C—D) bond, eQ the nuclear quadrupole moment, and $S = \frac{1}{2}<3\cos^2\alpha - 1>$ the degree of orientational order of the C—D bond direction with respect to the magnetic field. It can be seen from Eq. (5) that the resonance frequency depends on the orientation of the magnetic field in the principal axis frame (director frame) of the phase. In the case of macroscopically aligned samples, only two absorption lines are expected. This is the situation in the bulk nematic phase where the director is aligned in the magnetic field. In the case where samples are not uniformly aligned in an external field, a spectral distribution will result that will reflect the configuration of the directors in the sample.

A. Planar radial configuration

This case is trivial when the cylinder axes are parallel to the magnetic field since the directors are perpendicular everywhere to the magnetic field. This results in two singularities that correspond to the contribution from molecules with their principal axis oriented at an angle $\theta = 90°$. The quadrupole splitting in this case is one half of the aligned bulk nematic splitting as illustrated in Fig. 2(a). In the case where the cylinder's axes are oriented perpendicular to the magnetic field, the angle θ is uniformly distributed in a cylindrical distribution and the spectral pattern is illustrated in Fig. 2(c). This is the classical ^{2}H NMR spectral pattern for a cylindrical distribution and is similar to the spectral pattern obtained for a cholesteric phase where the pitch axis is perpendicular to the magnetic field.[11]

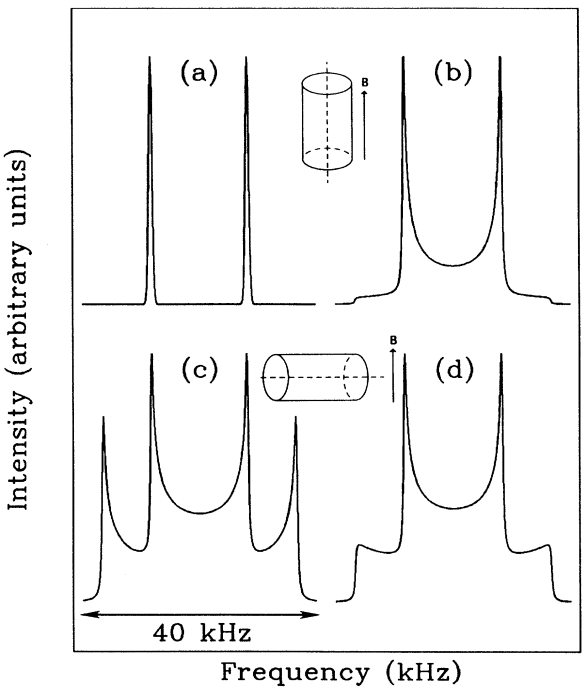

FIG. 2. Simulated ^{2}H NMR line shapes for nematic liquid crystal confined to cylindrical cavities with homeotropic type boundary conditions: the case of planar radial configuration (a) and the escaped-radial configuration (b), where the long axes of the cylinders are parallel to the magnetic field; planar radial (c) and the escaped-radial (d), where the long axes of the cylinders are perpendicular to the magnetic field.

B. Escaped-radial configuration

In this case, the spectral distribution $dN/d\omega_q$ can be calculated by the expression

$$\frac{dN}{d\omega_q}=\frac{dN}{d\rho}\frac{d\rho}{d\omega_q}\propto\rho\frac{d\rho}{d\omega_q}\ , \tag{6}$$

where N is the NMR signal intensity and ρ is expressed by Eqs. (3) or (4). For the case of equal deformation constants ($K_{11}=K_{33}$), the positive and negative contributions of the spectral pattern are given by

$$\frac{dN}{d\omega_q}\propto\frac{1}{(\sqrt{1\pm2x}+\sqrt{3})^2\sqrt{1\pm2x}}\ , \tag{7}$$

where $x=\omega_q/\pi\delta\nu$. A spectral simulation of Eq. (7) using Gaussian line broadening is illustrated in Fig. 2(b). It is characterized by two shoulders and two edge singularities. The singularities correspond to the contribution from molecules whose principal axis frame is oriented at an ange $\theta=90°$ and the orientation with $\theta=0°$ contributes to the intensity at the shoulders.

In the case where the cylinder's axes are orientated perpendicular to the magnetic field, the escaped-radial configuration yields a spectrum given by

$$\frac{dN}{d\omega_q}\propto\int_0^R\frac{\cos^2\phi}{\sqrt{(1\pm2x)}[\cos^2\phi-\frac{1}{3}(1\pm2x)]}\rho\,d\rho\ , \tag{8}$$

where $\cos^2\phi=4\rho^2R^2/(R^2+\rho^2)^2$ from Eq. (3). Performing the integration on Eq. (8), a complicated analytical expression is obtained. The calculated spectral distribution is shown in Fig. 2(d). This is similar to the cylindrical spectral pattern, except the intensity of the $\theta=0°$ singularities is smaller due to the escaping of the directors in the center of the cylinder.

The influence of the magnetic field can be included in the spectral line-shape calculation through Eq. (1). Two spectra have been calculated for the escaped-radial configuration in cylinders of size 0.3 μm in radius. Figure 3(a) illsutrates the case where the ratio of the magnetic coherence length and the radius of the cylinder is $\xi/R=\infty$ which corresponds to a null value for the magnetic field. The spectrum in this case essentially reduces to the static line shape calculated in Fig. 2(b). In Fig. 3(b) we have included a large, exaggerated value of the magnetic field ($B=26T$) for $\xi/R=1$. It can be seen that such a magnetic field did not influence the spectrum. Therefore, the NMR magnetic field of 4.7 T has no appreciable influence on the spectral line shape. The cylinder size has to be on the order of 2 μm for the field to influence the nematic director configuration for the quadrupole interaction studied.

C. Escaped-radial configuration with singular point defects

Theoretical spectra have been calculated for the escaped-radial configuration with singular point defects for the case where the cylinder axes are parallel to the magnetic field. This takes into account the encounter of two opposing escaping domains. This structure is illustrated in Fig. 1(d) where the point defects are incorporated by including radial planes separated by a distance L. There is no analytical expression in closed form between θ and ρ for the molecular distribution of this configuration. The spectrum is numerically calculated from Eq. (1) in the one-constant ($K_{11}=K_{33}$) approximation and shown in Fig. 4 for several different defect densities.[10] It is evident that the spectral line shape depends on the defect density expressed as the ratio L/R. For the case when $L/R=5.0$, shoulders corresponding to $\theta=0°$ become more apparent and the central portion of the pattern becomes enhanced in comparison to smaller L/R values.

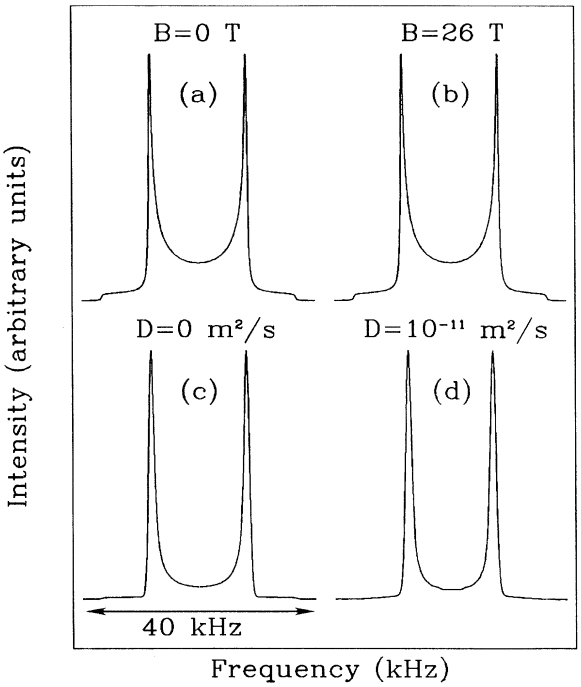

FIG. 3. Simulated ^{2}H NMR line shapes showing the influence of the magnetic field for a cylinder of radius 0.3 μm in the case of no magnetic field, $\xi/R=\infty$ (a), compared with a strong magnetic field, $\xi/R=1$ (b), the influence of diffusion in the case of negligible diffusion (c), compared with the line shape calculated for a typical diffusion constant $D=1\times10^{-11}$ m^2/s on the escaped-radial pattern with defects $L/R=1.5$ (d).

D. Self-translational diffusion

As argued earlier, the effect of translational diffusion is not expected to influence the spectral shapes because of the large quadrupole interaction. We have nevertheless included diffusion in the spectral pattern calculation for the case of the escaped-radial structure with point defects where diffusion would be expected to have the largest effect. The frequency spectrum for a deuteron pair is given by[12]

$$I(\omega)=\int_{-\infty}^{\infty}G(t)\exp(i\omega t)dt\ , \tag{9}$$

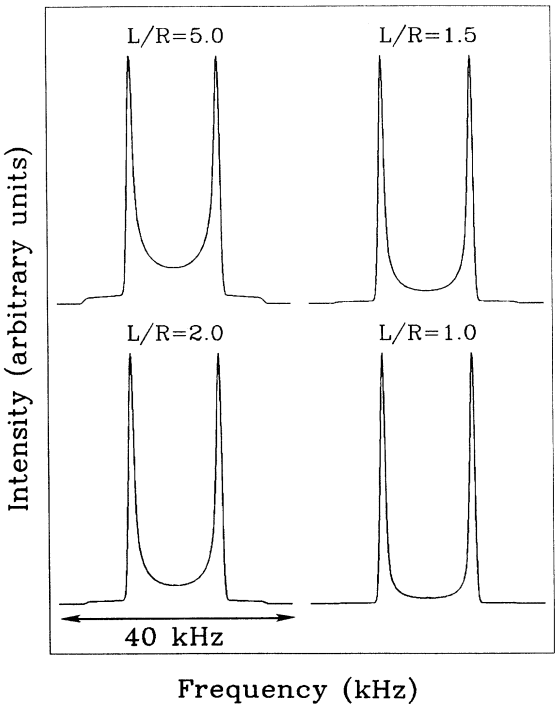

FIG. 4. Simulated ^{2}H NMR line shapes for the escaped-radial configuration with singular point defects for various densities (L/R) and cylinders whose long axes are parallel to the field.

where $G(t)$ is the autocorrelation function given by the relation

$$G(t)=\left\langle \exp\left[i\int_0^t \omega_q[\mathbf{r}(t')]dt' \right] \right\rangle , \tag{10}$$

where $\omega_q[\mathbf{r}(t)]$ is the instantaneous value of the quadrupolar frequency given by Eq. (5). Line broadening is taken into account by convoluting $I(\omega)$ with a gaussian distribution curve. A simple random jump model was employed to simulate the diffusion process, where a square lattice is introduced in the cylindrical cavity with a lattice spacing a. The molecules are allowed to "jump" with the same probability to one of the six nearest lattice sites. The "jump" time τ is given by $a^2/6D$, and reflection is assumed at the surface. This diffusion model has been previously employed in nematic microdroplets.[13] Figures 3(c) and 3(d) are calculated spectra with a defect density of $L/R=1.0$ for the static and dynamic ($D=1\times10^{-11}$ m^2/s) cases, respectively, for a cylinder of radius 0.3 μm. This verifies that diffusion has a minimal effect on the line shape for the larger cavity sizes. The diffusion is demonstrated only in a slight approach of the two main peaks.

IV. EXPERIMENTAL METHOD

The cylindrical cavities of polycarbonate Nuclepore membranes[14] are permeated with the liquid crystalline material 4'-pentyl-4-cyanobiphenyl (5CB-βd_2) deuterated

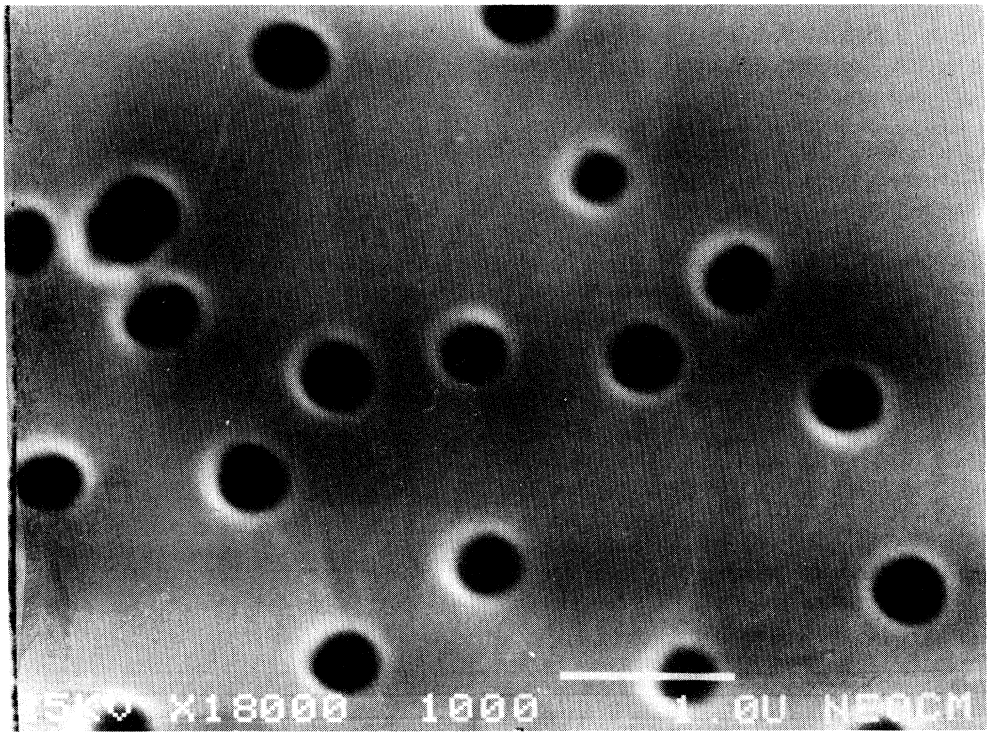

FIG. 5. Scanning electron microscope (SEM) photograph of a polycarbonate nuclepore membrane with pores of radius 0.3 μm.

in the β position of the hydrocarbon chain. Two pore sizes were employed, 0.3 and 0.2 μm in radius. The membranes were cut into 4-mm-wide strips and wetted with a small amount of 5CB-βd_2. The membranes were then placed in the oven for approximately 1 h at 40 °C to insure complete wetting of the porous cavities. They were removed from the oven and pressed between two Whathan filtration papers to remove the excess liquid crystal from the surface. Approximately 200 strips were uniformly stacked and placed in a 5-mm Norell precision thin-walled NMR tube. We estimated that the amount of liquid crystal material that remains on the surface of the membranes is negligible compared to that confined in the cavities.

Nuclepore membranes are polycarbonate filters used principally in critical filtration procedures requiring low absorption. The pores of the membranes are well-defined channels produced by using an irradiation-and-etching process. Specific pore sizes of a desired dimension are obtained by controlling the length of the etching process. These polycarbonate membranes have been used for many years in low-temperature physics laboratories in the study of superfluid helium, specifically to achieve a well-defined confined geometry to study finite-size effects near the superfluid transition.[15] Figure 5 shows a scanning electron microscope (SEM) photograph of a polycarbonate nuclepore membrane with 0.3-μm radius cylindrical pores. The high density of pores and the uniformity of the pores allows confinement studies of liquid crystals to be accessible with ^{2}H NMR. Various measurements have been made on Nuclepore membranes to characterize their heat capacity, pore size, and pore density.[15]

The experiments were performed on a home-built coherent pulse spectrometer interfaced through a Biomation 2805 digitizer to a Digital Equipment Corporation LSI-11/73 computer. A modified quadrupolar echo sequence ($\pi/2$-τ-$\pi/2$) was employed where τ was 100 μs and the length of $\pi/2$ pulse was 5 μs. The free-induction decay (FID) was averaged 10 000 times to achieve a reasonable signal-to-noise ratio. The digitized FID is 2000 points and the Fourier transform is computed over 4000 points by zero filling the additional 2000 points. The temperature is regulated by a circulating fluid bath with resolution of 0.1 °C and stability in the sample of 0.05 °C. The temperature is directly recorded from the sample chamber in the probe head through a platinum resistor connected to a resistance measuring device. The orientation of the sample about the axis perpendicular to the magnetic field is automated with a stepper motor with 0.05° resolution in θ_0. The sample is placed in the NMR magnet such that the long axis of the cylinders is parallel to the field and can be rotated through 90° such that the long axis of the cylinders is perpendicular to the magnetic field.

V. EXPERIMENT AND COMPARISON WITH THEORY

Figure 6 shows the ^{2}H NMR spectra for two orientations of the long axes of the cylinders with respect to the magnetic field. Figure 6(a) is the case where the long axes of the cylinders are parallel to the magnetic field. This

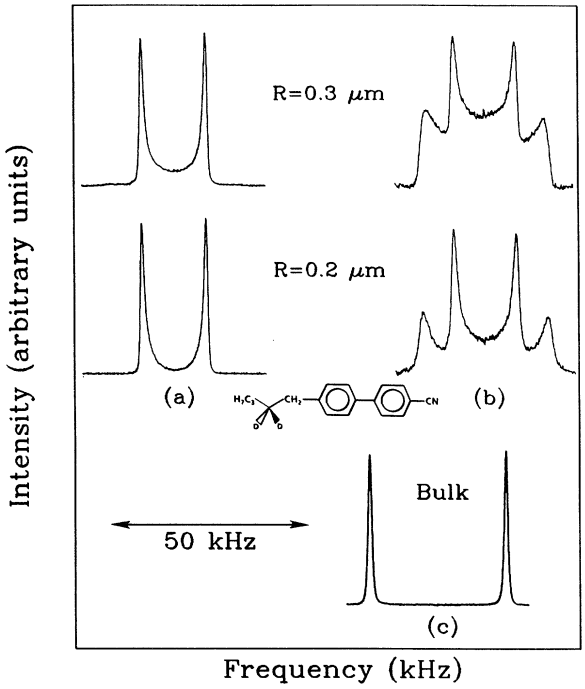

FIG. 6. Experimental ^{2}H NMR line shapes recorded at 24 °C for long axes of the cylinders parallel to the magnetic field (a), long axes of cylinders perpendicular to the magnetic field (b), and macroscopically aligned bulk 5CB-βd_2 sample (c).

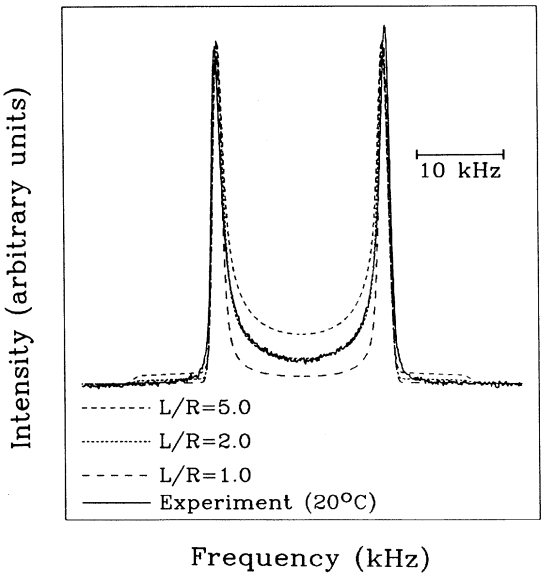

FIG. 7. Experimental spectrum at 20 °C from Nuclepore membranes with pores of radius 0.3 μm compared with theoretical line shapes for the escaped-radial configuration with singular point defects. $L/R=2.0$ gives the best fit.

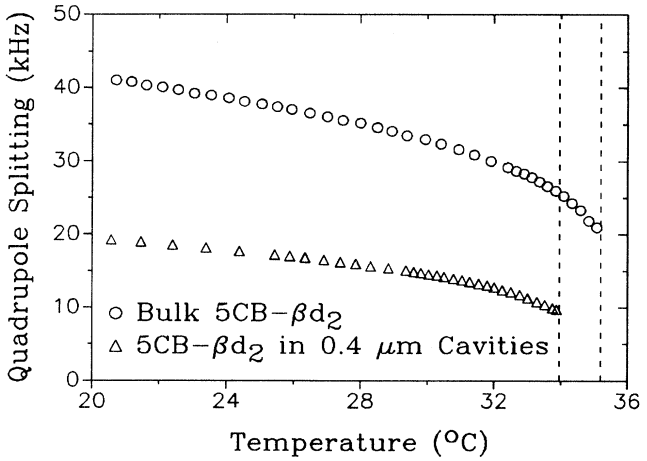

FIG. 8. Temperature dependence of the ^{2}H NMR quadrupolar splitting for the spectral lines of the aligned bulk 5CB-βd_2 material and the singularities of the spectral patterns for the confined 5CB-βd_2 material.

pattern is indicative of the escaped-radial configuration shown in Fig. 2(b), except the absence of a shoulder on the spectrum suggests that the configuration is of the escaped-radial type with singular point defects as illustrated in Fig. 1(d). When the long axis of the cylinders is oriented at 90° with respect to the magnetic field, a cylindrical-type powder pattern is obtained for both cylinder sizes plotted in Fig. 6(b). Figure 6(c) is the spectrum for a macroscopically aligned bulk 5CB-βd_2 sample.

Figure 7 is a direct comparison with theory for various values of L/R in a cylinder of radius 0.3 μm. The best fit is obtained for an average density of $L/R \simeq 2.0$ which is above the critical value $L/R \approx 0.25$ where the domain walls become attractive. There were several attempts to vary the cooling rate from the isotropic phase to investigate its influence on the density of point defects. The relative height of the central region of the spectrum is independent of the cooling rate when the sample is in the magnetic field, suggesting that the singular point defects are a consequence of the elastic energy and not the preparation method.

The temperature dependence of the 0.2-μm-radius membranes permeated with 5CB-βd_2 is shown in Fig. 8. The quadrupole splitting decreases as we approach the nematic-isotropic phase transition, which is expected. The temperature depression is expected to be largely a consequence of impurities effects introduced by the membrane and to a lesser extent on finite-size effects.

VI. CONCLUSIONS

The escaped-radial configuration with point defects on the escape axis is seen to be present in submicron-size cylindrical cavities with a radius as small as 0.2 μm. The observed defect density of $L/R = 2$ is consistant with predictions.[10] The prediction of Cladis and Kleman[2] that this configuration will revert to the planar radial configuration at $R \simeq 0.1$ μm has yet to be examined but is well within the realm of the ^{2}H NMR technique reported here, and is the subject of future work.

It should be mentioned that previous workers have assumed the strong anchoring case, which may not hold for very small values of R, in view of the recent study of nematic liquid crystals confined to spherical cavities by Erdmann *et al.*[8] In that work it was found that for small enough spherical droplets, the splay elastic energy imposed by the confining spherical cavity will compete with surface anchoring energies to alter the anchoring angle and induce a new configuration. Such a case could also occur in cylindrical cavities and is also a subject of future study.

The power and convenience of ^{2}H NMR in studies of confinement or finite-size effects on nematic liquid crystalline materials is clearly illustrated. It may be necessary in smaller geometries to include effects of diffusion. In geometries with radii larger than 1 μm, the affect of the magnetic field imposed by the NMR spectrometer would need to be included in the calculation of director configurations. In the cavity sizes used in this study, both diffusion and field effects can be neglected for the strength of the quadrupole interaction used. It is the subject of future work to explore configurations in the same cavity sizes with different preparations of the cavity surface for different anchoring angles and strengths.

ACKNOWLEDGMENTS

The authors wish to acknowledge support of the National Science Foundation under Solid State Chemistry Grant No. DMR88-17647. The deuterated compound 5CB-βd_2 was synthesized by Mary Neubert and Sandra Keast, whose work was supported under the Solid State Chemistry Grant No. DMR88-18561. The preliminary diffusion calculations were done by Samo Kralj.

*Permanent address: J. Stefan Institute, Jamova 39, Ljubljana, Yugoslavia.

[1]E. Dzyaloshinskii, Zh. Eksp. Teor. Fiz. **31**, 773 (1970) [Sov. Phys.—JETP **33**, 733 (1970)].
[2]P. E. Cladis and M. Kleman, J. Phys. **33**, 591 (1972).
[3]R. B. Meyer, Philos. Mag. **27**, 405 (1973).
[4]C. Williams, P. Pieranski, and P. E. Cladis, Phys. Rev. Lett. **29**, 90 (1972).
[5]C. E. Williams, P. E. Cladis, and M. Kleman, Mol. Cryst. Liq. Cryst. **21**, 355 (1973).
[6]P. G. deGennes, *The Physics of Liquid Crystals* (Clarendon, Oxford, England, 1974).
[7]M. Kuzma and M. M. Labes, Mol. Cryst. Liq. Cryst. **100**, 103 (1983).
[8]J. H. Erdmann, S. Žumer, and J. W. Doane, Phys. Rev. Lett. **64**, 1907 (1990).
[9]D. Melzer and F. R. NaBarro, Philos. Mag. **35**, 901 (1977).
[10]M. Vilfan, I. Vilfan, and S. Žumer (unpublished).
[11]C. Chidichomo, Z. Yaniv, N. P. Vaz, and J. W. Doane, Phys. Rev. A **25**, 25 (1982).

[12]A. Abragam, *The Principles of Nuclear Magnetism* (Clarendon, Oxford, England, 1962).
[13]S. Kralj, M. Vilfan, and S. Žumer, Liq. Cryst. **5**, 1489 (1989).
[14]Nuclepore Corporation, 7035 Commerce Circle, Pleasanton, CA 94566.
[15]T. P. Chen, M. J. DiPirro, B. Bhattacharyya, and F. M. Gasparini, Rev. Sci. Instrum. **51**, 846 (1980).

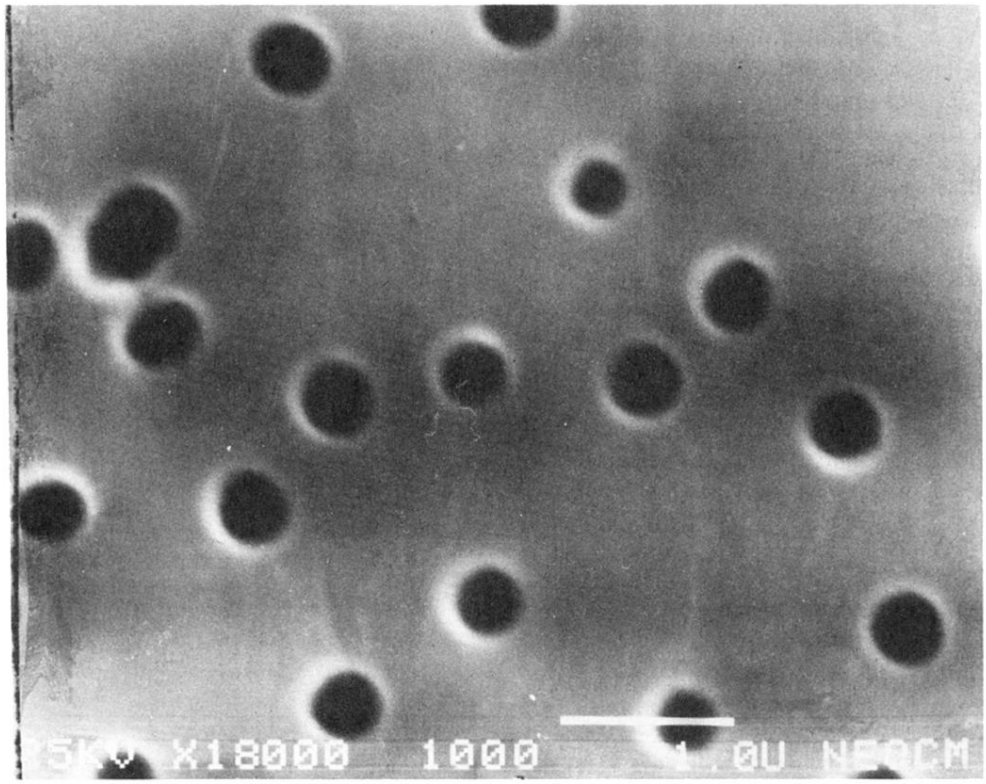

FIG. 5. Scanning electron microscope (SEM) photograph of a polycarbonate nuclepore membrane with pores of radius 0.3 μm.